

Article

An Investigation of Ice Surface Albedo and Its Influence on the High-Altitude Lakes of the Tibetan Plateau

Jiahe Lang ^{1,2} , Shihua Lyu ^{3,4}, Zhaoguo Li ^{1,*}, Yaoming Ma ^{2,5,6} and Dongsheng Su ^{1,2}

¹ Key Laboratory of Land Surface Process and Climate Change in Cold and Arid Regions, Northwest Institute of Eco-Environment and Resources, Chinese Academy of Sciences, Lanzhou 730000, China; langjiahe@itpcas.ac.cn (J.L.); sds@lzb.ac.cn (D.S.)

² University of Chinese Academy of Sciences, Beijing 100049, China; ymma@itpcas.ac.cn

³ Plateau Atmosphere and Environment Key Laboratory of Sichuan Province, School of Atmospheric Sciences, Chengdu University of Information Technology, Chengdu 610225, China; slu@cuit.edu.cn

⁴ Collaborative Innovation Center on Forecast and Evaluation of Meteorological Disasters, Nanjing University of Information Science & Technology, Nanjing 210044, China

⁵ Key Laboratory of Tibetan Environment Changes and Land Surface Processes, Institute of Tibetan Plateau Research, Chinese Academy of Sciences, Beijing 100101, China

⁶ CAS Center for Excellence in Tibetan Plateau Earth Sciences, Chinese Academy of Sciences, Beijing 100101, China

* Correspondence: zgli@lzb.ac.cn; Tel.: +86-0931-4967-239

Received: 22 November 2017; Accepted: 30 January 2018; Published: 1 February 2018

Abstract: Most high-altitude lakes are more sensitive to global warming than the regional atmosphere. However, most existing climate models produce unrealistic surface temperatures on the Tibetan Plateau (TP) lakes, and few studies have focused on the influence of ice surface albedo on high-altitude lakes. Based on field albedo measurements, moderate resolution imaging spectrometer (MODIS) albedo products and numerical simulation, this study evaluates the ice albedo parameterization schemes in existing lake models and investigates the characteristics of the ice surface albedo in six typical TP lakes, as well as the influence of ice albedo error in the FLake model. Compared with observations, several ice albedo schemes all clearly overestimate the lake ice albedo by 0.26 to 0.66, while the average bias of MODIS albedo products is only 0.07. The MODIS-observed albedo of a snow-covered lake varies with the snow proportion, and the lake surface albedo in a snow-free state is approximately 0.15 during the frozen period. The MODIS-observed ice surface (snow-free) albedos are concentrated within the ranges of 0.14–0.16, 0.08–0.10 and 0.10–0.12 in Aksai Chin Lake, Nam Co Lake and Ngoring Lake, respectively. The simulated lake surface temperature is sensitive to variations in lake ice albedo especially in the spring and winter.

Keywords: surface albedo; snow and ice; MODIS; lake model; parameterization scheme

1. Introduction

The Tibetan Plateau (TP) contains numerous lakes with a total area of 4.7×10^4 km² [1], and approximately 389 lakes are larger than 10 km² [2]. Over the past 82,000 years, there has been a good correlation between the shrinking of lakes in the TP and the weakening of the Asian monsoon [3]. In a global warming context, lake areas and water levels generally show an increasing trend, because of the increases in precipitation and glacier melt water that have occurred in the TP, while the lake ice-cover duration shows an overall decline [4–7]. Land surface temperature (LST) is the key factor regulating the exchange of energy and water in the air–lake interface [8]. In the TP, a few studies have shown that the LST rises even faster than regional air temperature in summer [9]. These lakes are located on the

third pole of the Earth, where the cold climate leads to a long frozen period (four to six months) for the TP lakes [10]. Recent studies have shown that shortening of the frozen period can lead to the earlier establishment of the summer thermocline in large and deep lakes, which accelerates the warming of the upper lake water [11–13]. Ice cover can increase the lake surface albedo and attenuate absorbed solar radiation, and thus strongly alters the significance of sensible and latent fluxes exchange as well as evaporation [14]. The freezing date of a lake is significantly affected by the lake's heat storage, while the melting of lake ice is mainly determined by solar radiation [15], particularly the solar radiation absorbed by the ice and the water.

The albedo is one of the main parameters in climate models [16] and regulates the surface energy budget. Previous studies have shown that lake ice and snow albedos generally range from 0.10 to 0.60 and from 0.50 to 0.95 [17–23]. Based on MODIS albedo products (MCD43A3, MOD10A1/MYD10A1) and field observation data, researchers investigated the ice surface albedo of Malcolm Ramsay Lake in Canada (with little snow cover), and found that it was greater than 0.6; moreover, the error of MCD43A3 product was smallest [24]. However, lake ice albedo less than 0.2 has only been reported by a handful of studies [17,25].

The huge spread in lake ice albedo values reported by different studies implies that an accurate ice albedo parameterization is necessary for weather and climate modelling. Lake ice albedo is related to a number of factors, such as solar zenith angle [26,27], ice type (white ice, snow ice, blue ice, etc.) [28], bubble content, ice thickness [29,30], the presence of impurities [20] and cloud cover [27]. There are three types of ice surface albedo schemes in lake models and coupled climate models. The first type is a specified constant, such as that used in the weather research and forecasting model (WRF). The second type is a function of ice surface temperature, like that used in the FLake model. The third type is more complex and takes into account snowfall, snow/ice thickness or other factors. The Canadian lake ice model (CLIMo) uses this type of parameterization scheme. Most ice albedo parameterization schemes in lake models are developed based on the early observations on high-altitude sea or lakes of the Arctic, and a few schemes are even derived from sea ice models. The ice is very thick and is often covered with snow in Arctic, which is quite different from that in the TP. The original observation data employed by the temperature-dependent albedo schemes, temporally averaged quantities as daily means or monthly means [31], are very discrete. The correlation between ice surface temperature and ice albedo is very low. It is impossible to characterize the effect of rapidly changing ice temperatures (like diurnal variations) on ice albedo. These parameterizations are not suitable for lake ice on the TP [32,33].

In northern Europe and North America, the climate is relatively humid, and the lake surface is often covered with snow during the frozen period. The impact of ice albedo error on lake simulation is largely offset by the snow cover. However, little precipitation falls over the arid and semi-arid TP during the frozen period, and there is often little or even no snow cover on the ice surface. Inaccurate estimation of ice albedo may lead to an obvious bias in the LST simulation in the coming year, subsequently affecting the regional climate modelling [24,31]. Mallard et al. [34] significantly improved the simulation of Great Lakes temperatures and ice cover through progressing the ice albedo parameterizations. However, little attention has been paid to the ice albedo of TP lakes. Only a few studies have analyzed the changes in the freezing date of Nam Co Lake [35], as well as lake ice structure [36], thermal conductivity [37] and ice melting [38] in a small TP thermokarst lake. Although the observation of lake ice albedo is quite scarce in the TP, the MODIS albedo products, which have a relatively small error, can help us to obtain an in-depth understanding of the ice albedo characteristics of a large lake.

In this study, the ice surface albedo parameterization schemes in existing models and the observation data are used to investigate the bias of ice albedo values in the model. The long-term MODIS albedo products are employed to analyze the characteristics of the surface albedo on TP lakes during the frozen period, and the FLake model is used to illustrate the effects of the inaccurate albedo parameterizations of the model.

2. Study Area, Data and Method

2.1. Study Area and In-Situ Measurements

Six typical lakes (Figure 1) with different surface areas (184.9–4254.9 km²), altitudes (3260–4990 m), depths and geographic locations, are selected to represent TP lakes (Table 1). Aksai Chin Lake, Nam Co Lake and Ngoring Lake will be analyzed as key targets in the following sections. Aksai Chin Lake, the highest (4848 m AMSL) and smallest lake (184.9 km²) of the six lakes, is still large enough to accommodate many MODIS 500-m resolution pixels. Nam Co Lake is the third-largest saline lake in the TP and the highest large lake on the earth. Ngoring Lake (4274 m AMSL), with a mean depth of 17 m and a surface area of 610 km², is the highest large freshwater lake in China, and it is located in the eastern TP.

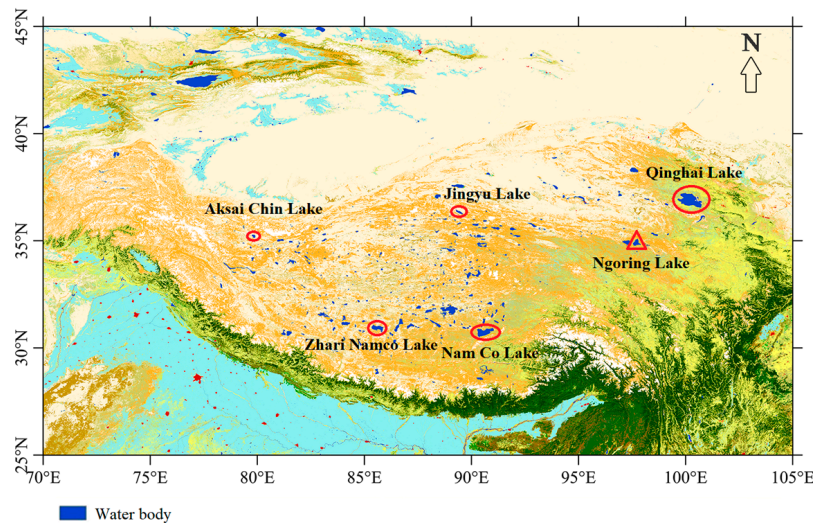


Figure 1. Locations of the six selected lakes. The triangle represents Ngoring Lake where the observations were carried out.

Table 1. Surface area and surface altitude of the six selected lakes.

Lake Names	Aksai Chin Lake	Nam Co Lake	Jingyu Lake	Zhari Namco Lake	Ngoring Lake	Qinghai Lake
Surface area (km ²)	184.9	2040.9	283.7	996.9	629.8	4254.9
Altitude (m)	4848	4718	4708	4613	4272	3260

From 3 to 6 January 2014, a short-term field experiment aimed at measuring the ice surface radiation balance was carried out over the west of Ngoring Lake (Figure 2a). The field observation was forced to terminate on 6 January due to a huge ice crack between the lakeshore and the observation site (34.92°N, 97.58°E). From 10 to 18 February 2017, an in-situ observation and another mobile observation of the ice albedo were performed over the west Ngoring Lake (Figure 2b). The maximum observation range is approximately 630 m in the meridional direction, and 960 m in the latitudinal direction. In this experiment, we obtained 529 groups of data from mobile albedo observation within 6 days (10:00–12:00 local time of every day), and diurnal measurements of a week from in-situ observation. During the observation period, patches of bare ice and snow cover were intermixed across the lake surface, but the bare ice was still dominant. The instrument used for these two observations is Kipp & Zonen 4-Component Net Radiometer (CNR4). The pyranometers and pyrgeometers measure shortwave (300–2800 nm) and long-wave infrared (4500–42,000 nm) radiation, respectively. The in-situ observation, at height of 1.20 m, measured once per minute and output a group of average data every 30 min, from 8:00 to 16:30. The mobile observation, at height of 1.60 m, measured once per 10 s and

output a group of average data every 60 s, from 11:30 to 13:30. The mobile albedo observation had a built-in global positioning system (GPS) sensor, which can record the instrument position in real time. The albedo α measured by pyranometers over the lake ice surface is obtained from the ratio $\alpha = \frac{S_{W\uparrow}}{S_{W\downarrow}}$, where $S_{W\uparrow}$ and $S_{W\downarrow}$ are the measured upward and downward shortwave irradiances, respectively. The observed long-wave radiation is used to calculate the ice surface temperature according to the law of Stefan–Boltzmann Equation (1).

$$Rl_{up} = (1 - \varepsilon)Rl_{dw} + \varepsilon\sigma T_0^4 \quad (1)$$

Here, σ ($=5.67 \times 10^{-8} \text{ W}\cdot\text{m}^{-2}\cdot\text{K}^{-4}$) is the Stefan–Boltzmann constant; Rl_{dw} and Rl_{up} are downward and upward long-wave radiations, and the ice surface emissivity ε is 0.99. T_0 is the ice surface temperature. The observed surface temperature will be used in the ice albedo parameterization scheme to obtain the model-derived albedo.



Figure 2. Observation platform in 2014 (a) and 2017 (b) on Ngoring Lake. In 2017, both of the in-situ and mobile observation platforms are presented.

2.2. Data

2.2.1. MODIS Albedo Products

The MCD43A3 V005 16-day albedo product, which combines albedo retrievals from the Terra and Aqua satellites, is used to analyze the characteristics of the surface albedo on TP lakes (October 2012 to June 2013, October 2013 to June 2014, and October 2014 to June 2015). It includes albedo measurements at a 500-m spatial resolution that is updated every 8 days [39]. The pixels that cover the six lakes are carefully selected (two pixels within the lake boundary are removed) to ensure that land contamination is not an issue. The MCD43A product used in this study is the White Sky Albedo (WSA) for the shortwave band (459–2155 nm) product. Svacina et al. [24] found that the snow and ice albedo obtained from MCD43A3 had a smaller error than MOD10A1 and MYD10A1 daily albedo products, compared with in-situ observations. MCD43A2 is the quality assurance product for MCD43A3, and it records whether the pixel has the snow-cover. This information will be used to calculate the ratio of the snow-covered to snow-free pixels on the lake surface. The MCD43A V005 product used in this study updates the value every 8 days. Daily MCD43A V006 products have been officially released and it is used to make a comparison with the mobile observation results. Daily MCD43A product is also a 16-day product that retrieves each day and utilizes all high-quality, multi-date, multi-angle, cloud-free surface reflectance from a rolling 16-day period in which the day of interest is defined as the centre date [2,40]. A brief discussion will be presented at the end of this study to reveal the difference between MCD43A-V005 and MCD43A-V006 (from October 2013 to June 2014).

The MOD10A1 product is used to consider percentage of snow-covered pixels of Aksai Chin Lake (1 to 16 January 2014), which includes the snow-covered albedo, snow cover proportion, quality information and other metadata at a spatial resolution of 500 m [31,41].

2.2.2. MODIS Surface Temperature Product

The MODIS land surface temperature product (MOD11A1) is used to evaluate the long-term simulated results in this study which covers 2012–2016 with a spatial resolution of 1 km. Many studies have shown that the MODIS land surface temperature product has good accuracy [9,42,43].

2.3. Lake Ice Albedo Parameterizations and the FLake Model

Many lake ice albedo parameterizations have been developed, and these schemes have varying degrees of complexity. The simplest scheme applies two or more constant values of albedo for different ice types. Some schemes (e.g., that used in FLake) add a dependence on temperature to account for the combined effects of LST. More sophisticated schemes (e.g., that used in CLIMo) also include the dependence of albedo on ice and snow thickness. The ice albedo scheme in FLake is derived from a thermodynamic sea ice model [44]. The ice surface albedo (α) in the FLake model is calculated as:

$$\alpha = \alpha_{max} - (\alpha_{max} - \alpha_{min}) \times \exp\left[-95.6 \times (T_{f0} - T_i) / T_{f0}\right] \quad (2)$$

where α_{max} is set to 0.6, referring to the albedo of white ice or snow ice. The blue ice albedo (α_{min}) is equal to 0.1. T_{f0} is the freezing temperature (273.15 K), T_i is the ice surface temperature. As the ice surface temperature (T_i) approaches the freezing temperature (T_{f0}), the albedo approaches 0.10. In the WRF model, the lake ice albedo is set to 0.6. The community land model (CLM) is the land surface model for the community earth system model (CESM). The lake model of CLM, denoted the lake, ice, snow, and sediment simulator (LISSS), is derived from Subin et al. [45] with one lake modelled in each grid cell. The CLM model distinguishes the lake ice albedo in different wavelength range of visible light and near infrared light. For frozen lakes without individually resolved snow layers, the albedo at cold temperatures α_{max} is 0.60 for visible radiation (CLM-max) and 0.40 for near infrared radiation (CLM-min). Therefore, the albedo parameterization scheme in CLM is similar to that used in FLake, evolving from Equation (2).

The 1-D FLake model is designed to simulate lake water temperature profiles and surface heat fluxes [46,47]. The FLake model is suggested to be applicable for freshwater lakes with depths of less than 60 m. Furthermore, a lake-ice layer, snow layer, and lake sediment layer are considered. Previous studies have shown that the FLake has been widely used and has a good performance [48–50]. In this study, we employed the FLake model to evaluate the influence of the ice albedo on lake simulation in Ngoring Lake. The simulation experiments begin in July 2011 and end in December 2016. The lake depth is set to be 25 m. The forcing data are derived from the observation in Ngoring Lake which is come from the Automatic weather station (AWS) built on the edge of the lake next to the observation area. The main input variables include the surface temperature, relative humidity, wind speed, air pressure, down short-wave and longwave radiations, precipitation from 1 July 2011 to 1 January 2017. The simulations begin in July 2011 instead of January 2012 for model spin-up.

3. Results

3.1. Albedo from MODIS, Observation and Parameterization-Driven

The four parameterization schemes (CLM4.5, FLake, WRF, and WRF-FLake) are evaluated against the in-situ observation collected in Ngoring Lake in 2014 and 2017 (Figure 3). The observed surface temperature is employed by these schemes to obtain the ice surface albedo. Of these schemes, the WRF-FLake model shows the maximum bias, followed by WRF and FLake. The albedo values derived from CLM4.5, especially CLM4.5_Min, are relatively closer to the observations. The schemes

in CLM4.5, FLake and WRF-FLake can reproduce the diurnal variation of albedo relatively well, but are significantly overestimated. Taking those of 2017 as an example, the model bias for FLake, CLM4.5, WRF and WRF-FLake range from 0.079 to 0.484, 0.177 to 0.485, 0.197 to 0.516 and 0.362 to 0.677, respectively. The maximum biases in four schemes appear at noon (12:00 in local time) which range from 0.26 to 0.66. Moreover, the diurnal pattern of simulated albedo is not a typical U-shaped curve as same as the observation. The lowest albedos from simulation appear at 13:30–15:00, but the observations remain almost unchanged from 11:00 to 15:00. This is because the aforementioned albedo schemes strongly depend on the ice surface temperature, and the latter has an asymmetric diurnal variation, with a maximum value at 13:30–15:00.

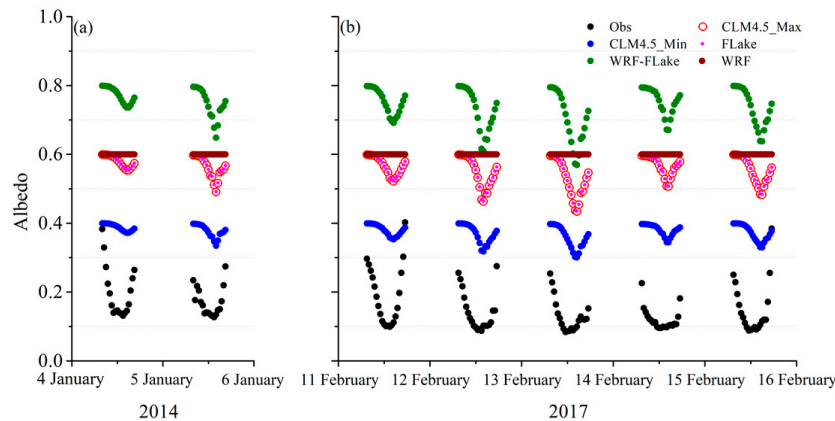


Figure 3. Lake ice albedos based on the in-situ observations and different albedo parameterization schemes in Ngoring Lake for 4 and 5 January 2014 (a) and 11 to 16 February 2017 (b) (local time).

The ice albedos from mobile observation in 2017 and snow-free MODIS product are presented in Figure 4. The mobile observation expands the spatial representation of ground observations and makes it easier to compare with MODIS product. Compared with the simulated values from different albedo parameterizations, the albedo from MODIS lies closest to the in-situ observations. The ice albedos from mobile observation range from 0.068 to 0.256, and are centered at 0.105. The MODIS observations range from 0.079 to 0.223, and are centered at 0.175. This means that the average bias of MODIS albedo products is only 0.07.

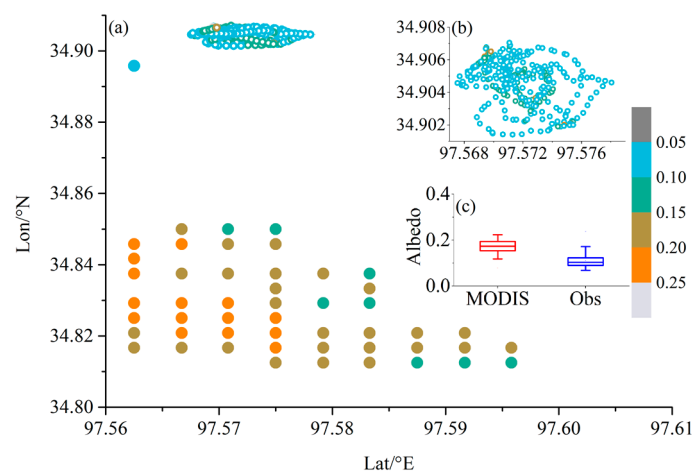


Figure 4. Colormap scatter plot of mobile observation and moderate resolution imaging spectrometer (MODIS) product values (a) and the enlarged view of the mobile observation (b) in Ngoring Lake from 11 to 18 February 2017, solid circles represent MODIS values in the figure, and open circles represent mobile observation (Obs) result; Their average distributions are presented in the Box graph (c).

3.2. Lake Surface Albedo Characteristics during the Frozen Period Derived from MODIS Observation

During most of the study period, the median values of albedo with snow cover are lower than 0.6 (Figure 5a, Figure 6a, Figure 7a). The albedos of different types of snow are different, which results in drastic changes in the albedo of the snow-covered lake. The surface albedo without snow cover remains relatively constant at approximately 0.18 in Aksai Chin Lake, 0.15 in Ngoring Lake and Nam Co Lake during the frozen period (Figure 5b, Figure 6b, Figure 7b). There are two peaks (approximately 0.5) in albedo with snow-cover in Ngoring Lake (Figure 6a), which coincide with a high proportion of snow-covered area (Figure 6c). All the surface albedos covered with snow in Nam Co Lake are higher than those from Aksai Chin Lake and Ngoring Lake during the same time. During periods with extensive snow cover, the albedos are higher, and the median value can reach 0.6 in Nam Co Lake (Figure 7a,c). In addition, the average albedo of the lake surface albedo is close to the snow-covered lake surface albedo because the snow cover area is much larger than the snow-free area during most of the study period.

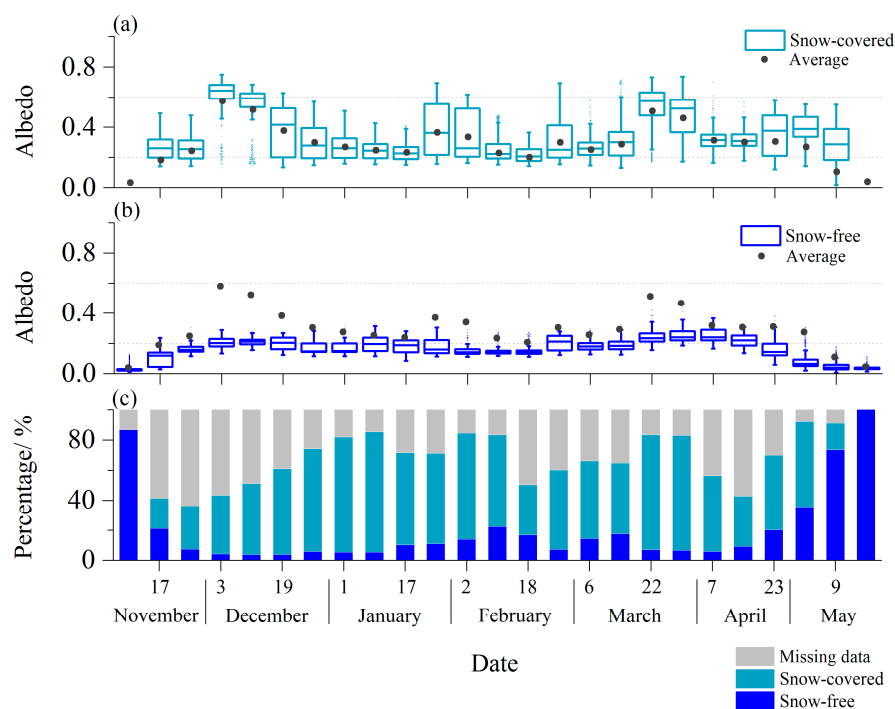


Figure 5. Snow-covered (a) and snow-free (b) surface albedo (box plots) in Aksai Chin Lake from 9 November to 17 May of the following year during three years. The black dots represent the average albedo derived from all available data (snow-covered and snow-free). The percentages of snow-covered, snow-free and missing data are shown in (c). The centre of each box represents the median value, the edges of each box indicate the 25th and 75th percentiles, and the whiskers represent the 5th and 95th percentiles of the distributions. The first line of tick labels in X-axis represents the date and the second line represents the month.

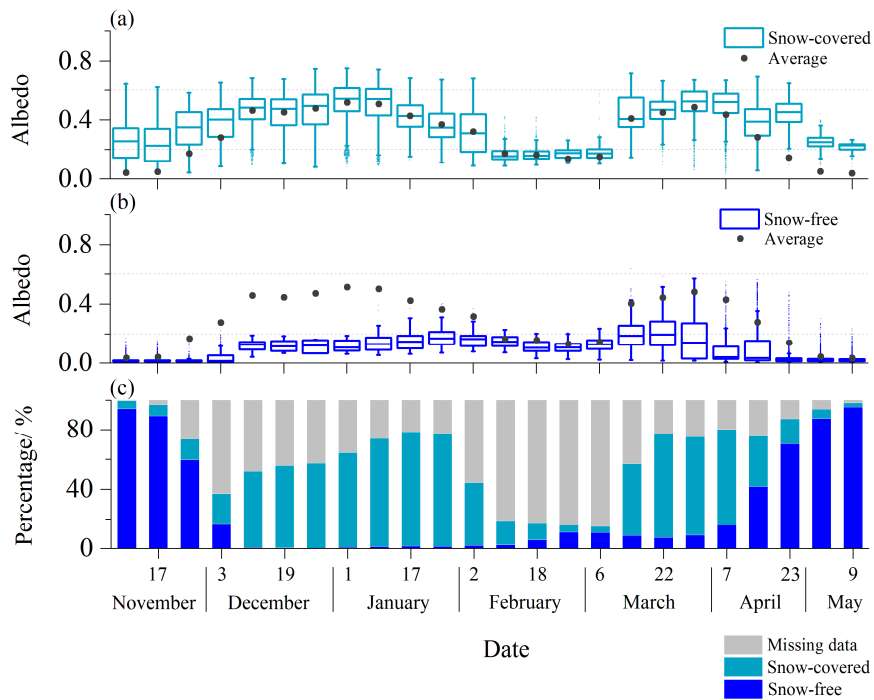


Figure 6. Snow-covered (a) and snow-free (b) surface albedo (box plots) in Ngoring Lake from 9 November to 9 May of the following year for three years. The black dots represent the average albedo derived from all available data (snow-covered and snow-free). The percentages of snow-covered, snow-free and missing data are shown in (c).

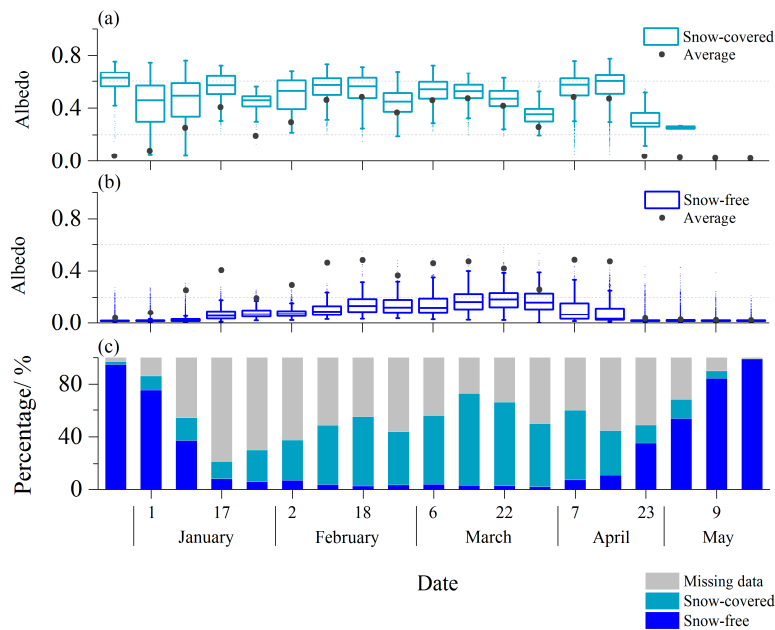


Figure 7. Snow-covered (a) and snow-free (b) surface albedo (box plots) in Nam Co Lake from 27 December to 17 May of the following year for three years. The black dots represent the average albedo derived from all available data (snow-covered and snow-free). The percentages of snow-covered, snow-free and missing data are shown in (c).

3.3. Distribution of the Albedo during the Frozen Period Derived from MODIS Observation

Table 2 summarizes the three-year average (from 2013 to 2015) of the monthly average albedo for the six lakes from October to June. The albedos of snow-covered lakes range from 0.12 to 0.54, and both of maximum and minimum values appear in Jingyu Lake, which has the longest snow-covered period that extends from late October to early June. When the ice covers more than 95% of the total lake area, this time is defined as the completely frozen period. The completely frozen period of Nam Co Lake in this study matches perfectly with the observations [51], which suggests that this determination method is reliable. Overall, the surface albedos with snow cover are relatively high in Nam Co Lake, Jingyu Lake and Zhari Namco Lake, especially from January to March, which range from 0.31 to 0.54, 0.12 to 0.51 and 0.23 to 0.4, respectively. The surface albedo values with snow-cover range from 0.23 to 0.35, 0.20 to 0.41 and 0.22 to 0.29 in Aksai Chin Lake, Ngoring Lake and Qinghai Lake, respectively. Take February for example, because February is the intermediate stage of the lake frozen period. Snow-free surface albedos of all lakes range from 0.14 to 0.3, which match perfectly with the observation obtained from the Great Lakes by Bolsenga [7] (0.1–0.46). Of these, the ice albedos are relatively small (0.14) in Nam Co Lake and Ngoring Lake (Table 2).

Table 2. Three-year average (from 2013 to 2015) of the monthly average of snow-covered and snow-free surface albedos for six selected lakes. “SD” means standard deviation.

Lake Names		Aksai Chin Lake	Jingyu Lake	Zhari Namco Lake	Ngoring Lake	Nam Co Lake	Qinghai Lake
Snow-covered	October	-	0.12	-	-	-	-
	November	0.23	0.32	0.23	0.22	-	0.22
	December	0.31	0.37	0.29	0.36	-	0.28
	January	0.25	0.40	0.40	0.41	0.40	0.29
	February	0.26	0.28	0.32	0.20	0.52	0.29
	March	0.35	0.44	0.27	0.38	0.54	0.23
	April	0.28	0.51	0.24	0.36	0.42	-
	May	0.27	0.47	-	0.23	0.31	-
	June	-	0.27	-	-	-	-
	Mean	0.28	0.35	0.29	0.31	0.44	0.26
SD	0.04	0.11	0.06	0.08	0.08	0.03	
Snow-free	October	-	0.02	-	-	-	-
	November	0.11	0.14	0.01	0.02	-	0.01
	December	0.21	0.21	0.03	0.10	-	0.05
	January	0.22	0.24	0.25	0.16	0.07	0.20
	February	0.20	0.20	0.30	0.14	0.14	0.16
	March	0.24	0.27	0.20	0.18	0.19	0.06
	April	0.22	0.34	0.05	0.10	0.14	0.02
	May	0.08	0.25	-	0.02	0.05	-
	June	-	0.04	-	-	-	-
	October	-	0.12	-	-	-	-
Mean	0.18	0.18	0.14	0.10	0.12	0.08	
SD	0.06	0.10	0.11	0.06	0.05	0.07	

The probability distributions of the albedo in three lakes are presented in Figure 8. The peaks of the snow-free surface albedo are concentrated within the ranges of 0.15–0.20, 0.10–0.15 and 0.10–0.15 in Aksai Chin Lake, Nam Co Lake and Ngoring Lake, respectively, which are close to those of clear ice [7]. When all the data are included, the albedo is still centered around the peak value of 0.20 in Aksai Chin Lake, and the low albedo samples are dominant. Conversely, compared with snow-free surface (Figure 8b), there is an obvious offset in the peak of albedo (0.55–0.60) derived from all data in Nam Co Lake (Figure 8e), and the low albedo samples only account for a small fraction. In contrast to the previously mentioned two lakes, the kurtosis of the peak significantly decreases in Ngoring Lake, and each interval has many samples from 0.10 to 0.65.

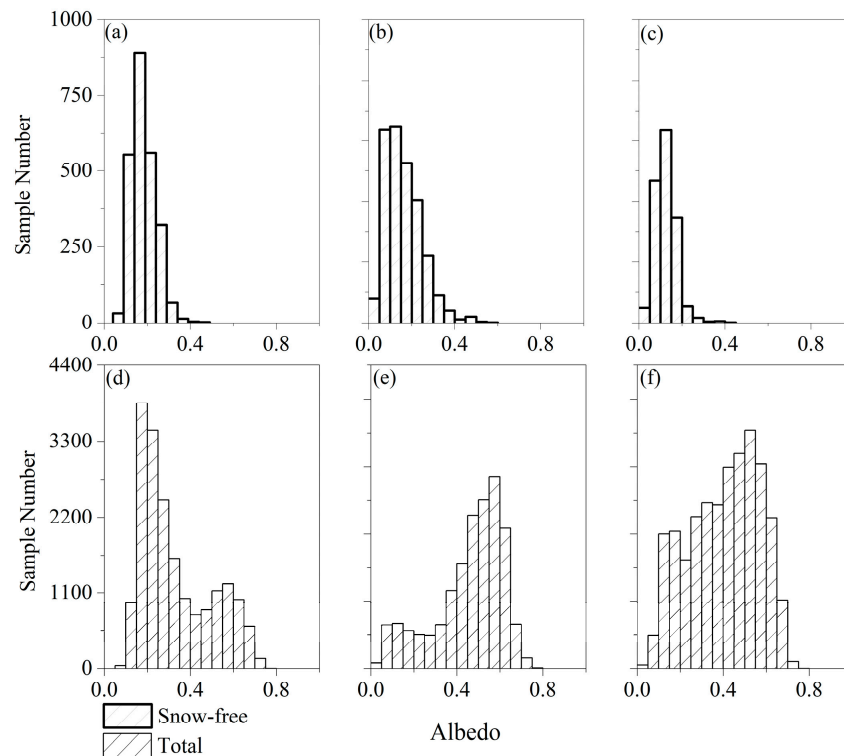


Figure 8. Probability distribution of the surface albedo in Aksai Chin Lake (a,d), Nam Co Lake (b,e) and Ngoring Lake (c,f) during the completely frozen period.

3.4. Influence of the Albedo Error in the Simulation with the Observation Data Derived from MODIS

The overestimated albedo means that less solar radiation is absorbed by the lake during the frozen period. As a result, it can significantly affect the timing of ice break-up in models [52–55]. Salonen et al. [56] found that the changes in solar radiation input can significantly affect the melting date of lake ice in the last two weeks of the frozen period. Van Cleave et al. [57] found that a drop in the ice duration can increase the water temperature in summer and the evaporation rates of July–August.

The effects of varying ice albedos (from 0.1 to 0.4) on LST, ice thickness and the dates of freezing and melting in FLake model are presented in Figure 9 and Table 3. When the ice albedo is set to 0.1, 0.15, 0.2 and 0.4, the root-mean-square error (RMSE) of LST (from 2012 to 2016) is 9.70, 9.78, 9.78 and 9.84 day, respectively. The RMSE of the FLake result is 10.17 day. At the same time, all results are well correlated with MODIS observations result with high correlation coefficient which is range from 0.95 to 0.96. The simulated LSTs are sensitive to variations in ice albedo especially from April to June (Figure 9). When the albedo ranges from 0.1 to 0.4, the LST can differ by up to 10 °C. The MODIS results almost coincide with the simulated results with low ice albedo in April and May. However, the MODIS results are significantly lower than the simulation values in June and July when the LST rose to 7 °C (Figure 10). It may be as the cool skin effect caused by wind speed after the lake ice is melted [58]. In a word, when the ice albedo is close to the mobile observation result (0.108) and MODIS observation result (from 0.1 to 0.15) in Ngoring Lake, the simulation results are more consistent with the MODIS observation results in melting period of Ngoring Lake (Figure 9).

Table 3 summarizes the effect of the ice albedo on lake ice phenology. The increasing albedo can consistently postpone the time of ice break-up in the simulations. When the albedo ranges from 0.1 to 0.4, the lake ice melting date will postpone for 10–43 days (2012–2016). When the albedo increases from 0.1 to 0.2, it postpones for 2–14 days, and when the albedo increases from 0.2 to 0.4, it postpones for 10–33 days. The average ice thickness increases with the increase in albedo. The averaged LST in the coming summer (from July to August) decreases with the increase of albedo (from 0.1 to 0.4), except 2012–2013. The averaged LSTs in winter (December to February of next year) generally show a decreasing trend with the increase of albedo, except in 2012–2013. However, the change in freezing date is irregular in different experiments, because it is also affected by the air temperature in the forcing data.

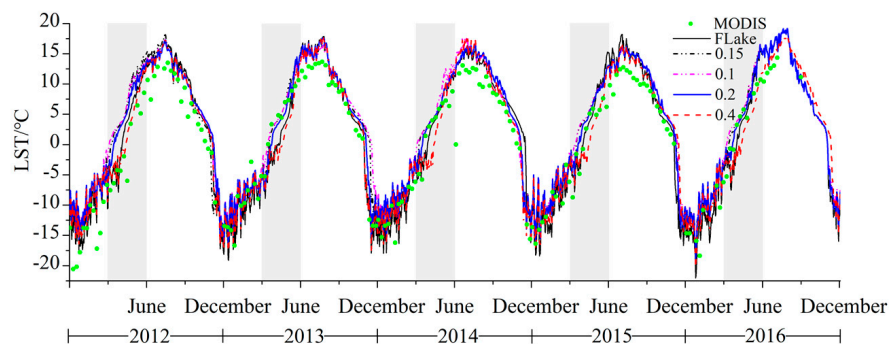


Figure 9. The land surface temperature (LST) from MODIS and the simulations in Ngoring Lake from 2012 to 2016; “FLake” means the simulation adopts the default ice surface albedo scheme in FLake, and the numbers “0.1, 0.15, 0.2, 0.4” mean the ice albedo is set to the corresponding value in FLake model; Shaded area indicates April to June (included).

Table 3. Lake ice phenology from simulated and MODIS observation (freezing date, melting date, ice thickness) and coming summer LST in Ngoring Lake.

Ice Duration	Albedo Parameterized	Freezing Date	Melting Date	Ice Thickness	Coming Summer LST	LST in Winter
2012–2013	0.1	5 December 2012	14 April 2013	0.48	15.11	−9.17
	0.15	30 November 2012	18 April 2013	0.56	15.44	−10.24
	0.2	8 December 2012	14 April 2013	0.54	15.87	−9.12
	0.4	5 December 2012	24 April 2013	0.69	15.68	−10.58
	FLake	5 December 2012	12 May 2013	0.74	16.04	−11.56
2013–2014	0.1	17 December 2013	2 April 2014	0.43	15.52	−7.49
	0.15	13 December 2013	8 April 2014	0.52	14.86	−8.35
	0.2	3 December 2013	16 April 2014	0.56	14.85	−9.53
	0.4	29 November 2013	15 May 2014	0.66	15.42	−11.36
	FLake	29 November 2013	28 April 2014	0.69	14.27	−12.58
2014–2015	0.1	2 December 2014	14 April 2015	0.5	14.33	−9.3
	0.15	5 December 2014	16 April 2015	0.54	14.31	−9.15
	0.2	6 December 2014	20 April 2015	0.57	14.4	−9.27
	0.4	4 December 2014	18 May 2015	0.66	13.99	−10.51
	FLake	16 December 2015	2 May 2015	0.67	14.96	−9.61
2015–2016	0.1	12 December 2015	6 April 2016	0.53	16.97	−9.17
	0.15	9 December 2015	11 April 2016	0.58	16.97	−9.61
	0.2	8 December 2015	20 April 2016	0.59	16.94	−9.91
	0.4	15 December 2015	11 May 2016	0.66	15.39	−9.92
	FLake	4 December 2015	30 April 2016	0.73	16.87	−12.93

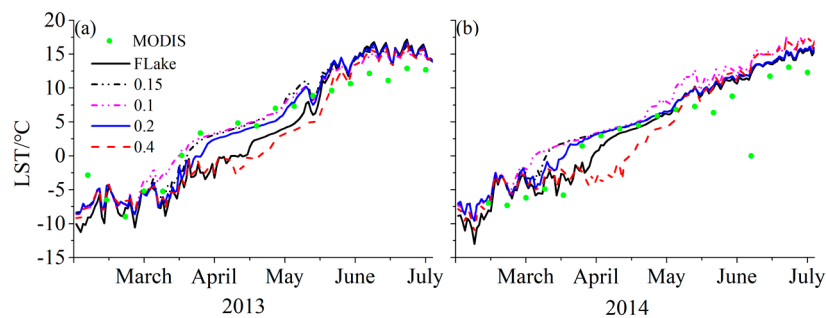


Figure 10. The LST from MODIS and the simulations in Ngoring Lake from March to July 2013 (a) and 2014 (b); “FLake” means the simulation adopts the default ice surface albedo scheme in FLake, and the numbers “0.1, 0.15, 0.2, 0.4” mean the ice albedo is set to the corresponding value in FLake model.

4. Discussion

We organized field observations to obtain the actual albedo of the lake ice, which confirmed that the parameterization scheme seriously overestimated the ice albedo on the TP lake (0.26–0.66). We proved the universality of low albedo (0.1–0.2) in TP lakes through the analysis of MODIS products in six typical TP lakes. A few albedo observations for the Great Lakes and high-altitude lakes have been reported [17,24,25]. However, these studies are rarely associated with lake ice albedo parameterization. As previously stated, the ice surface albedo can seriously affect the simulation of the lake ice-freezing period, and then indirectly affect the lake surface temperature in the ice-free period, as well as the regional weather and climate simulation. According to our simulation results, when the albedo changes from 0.1 to 0.4, the simulation results can differ by up to ten degrees at the same time, and the lake ice melting date was postponed for 10–43 days (2012–2016). At present, scholars pay less attention to the ice duration in TP lakes. Only a few studies analyzed the changes in the freezing date of Nam Co Lake [34], as well as lake ice structure [35], thermal conductivity [36] and ice melting date [37] in a small TP thermokarst lake.

What is interesting is that the significant impact of ice albedo on LST continues from mid-April to the end of June. Our further work will use the better remote sensing products, calibrated observation to improve the parameterization scheme of ice albedo, and make it more suitable for the TP lakes. We will also focus on more comprehensive simulation using the atmosphere-lake coupling model such as WRF. Then we will explore how much the different parametrization affects the results of the climate modelling in terms of impact on the main variables.

There remain a few uncertainties on MOD43A products. Figure 10 shows the surface albedo and the ratio of snow-covered to snow-free pixels based on the V005 and V006 MCD43A3 products in Aksai Chin Lake during the frozen period. Many models require daily albedos, especially during the ice/snow melting season when the snow/ice albedo changes rapidly [40]. Therefore, the new 16-day MODIS albedo products (V006) that is updated every day have been released, which helps to improve retrievals in high-altitude regions and can better capture conditions associated with snow cover and dormant vegetation [59]. The surface albedo under snow-free conditions in the V005 is almost the same as that in the V006 product (Figure 11a), which means the lake ice albedos used in the previous sections are in line with the results from V006 product. Compared with the V006, the ice albedo with snow cover in the V005 is higher from the 49th day to the 97th day of 2014. However, a paradoxical phenomenon appears from the 1st day to the 16th day of 2014. During this period, the percentage of snow-covered pixels is high, but the surface albedos only hover around 0.2 (Figure 11a). At that time, the normalized difference snow index (NDSI) within each pixel is also quite large, based on the MOD10A1 daily albedo product (Figure 12a). Correspondingly, the MOD10A1 product also presents a relatively small albedo that ranges from 0.1 to 0.3, except on the 6th day of 2014 (Figure 12b). Chen et al. [60] found that the albedo of MODIS MCD43 in the TP was mainly under the “snow-free” state. Therefore, this issue is universal on the TP. There may be some reasons, such as the MODIS product algorithm, which

lead to low albedos in highly snow-covered pixels during this period. However, the reason needs to be further explored in future work.

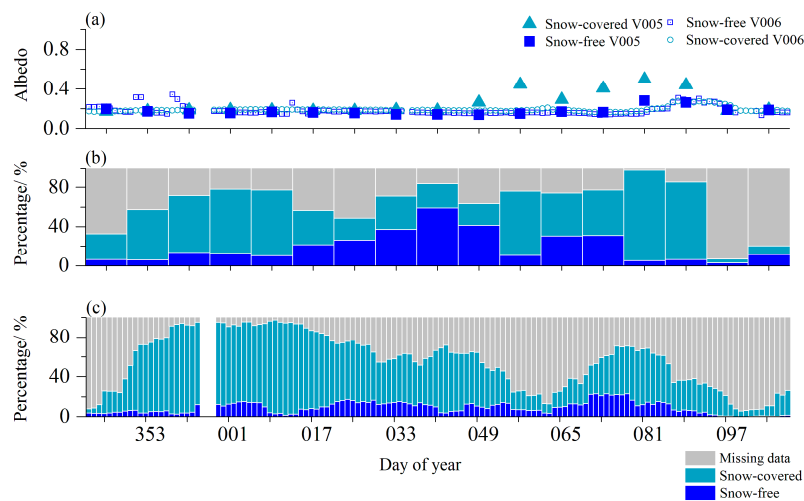


Figure 11. Lake surface albedos in Aksai Chin Lake from the 342nd day of 2013 to the 109th day of 2014, as derived from the V006 and V005 MCD43A3 products (a); and the ratio of snow-covered to snow-free pixels for the V006 (b) and V005 (c) products.

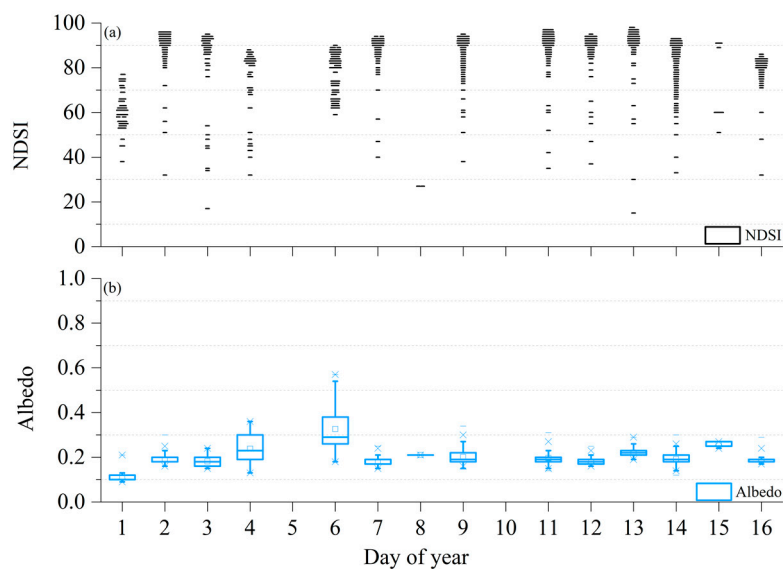


Figure 12. Surface albedo and normalized difference snow index (NDSI) (box plots) in Aksai Chin Lake (1 to 16 January 2014). (a) NDSI; (b) Surface albedo.

5. Conclusions

Using the observational data collected in Ngoring Lake in 2014 and 2017, the ice albedo parameterizations in existing lake models are evaluated in this study. The characteristics of surface albedo in six typical high-altitude lakes are investigated based on MODIS albedo products covering the lake ice phenology period from 2013 to 2015. Further, the effect of ice albedo on the lake simulation is evaluated using FLake model. The results can be summarized as follows.

Compared to observations, the albedo parameterization schemes in existing lake models tend to overestimate the ice albedo, with a bias of 0.26–0.66. In contrast, the albedos derived from MODIS coincide with the field-observed values well, with only a slight overestimation of 0.07. Different from

the typical U-shaped curve presented in the observation, the diurnal variations of simulated albedo are relatively irregular, and the minimum value lags behind the observation.

The surface albedos of Nam Co Lake, Jingyu Lake and Zhari Namco Lake are relatively high during the frozen period, ranging from 0.31 to 0.54, 0.12 to 0.51 and 0.23 to 0.4, respectively. The albedos of Aksai Chin Lake, Ngoring Lake and Qinghai Lake range from 0.23 to 0.35, 0.20 to 0.41 and 0.22 to 0.29, respectively. The albedo variation is closely related to the proportion of snow cover on the lake surface. Snow-free surface albedos range from 0.14 to 0.3 in February. The peaks of ice surface albedos in a snow-free state are concentrated within the ranges 0.14–0.16, 0.08–0.10 and 0.10–0.12 in Aksai Chin Lake, Nam Co Lake and Ngoring Lake during the completely frozen period, which are close to the albedo of clear ice.

The lake ice albedo has a significant effect on the melting date in spring and the minimum temperature of simulated LST in winter. When the albedos change from 0.1 to 0.4, the lake ice melting date is postponed for 10–43 days (2012–2016). Additionally, the simulation result is closest to the observation when the ice albedo is close to the observation (from 0.1 to 0.2) in the lake model. The averaged LST in winter and summer generally show a decreasing trend with the increase of lake ice albedo (from 0.1 to 0.4).

Acknowledgments: This study is supported by the National Natural Science Foundation of China (Nos. 41605011, 41775016, 41661144043, 91537104, 91637312), the Science and Technology Service Network Initiative of CAREERI (651671001), the Foundation for Excellent Youth Scholars of NIEER, CAS (Y651K51001), the Chinese Academy of Sciences (QYZDJ-SSW-DQC019). We acknowledge the hard work of Shaobo Zhang and Xiaohui Peng in the field observations. We thank American Journal Experts (AJE) English language editing for its assistance with the manuscript preparation.

Author Contributions: Shihua Lyu and Yaoming Ma conceived and designed the experiments; Zhaoguo Li, Jiahe Lang, and Dongsheng Su performed the experiments; Zhaoguo Li and Jiahe Lang analyzed the data; Jiahe Lang wrote the main manuscript, and all the authors contributed to write and discuss the paper.

Conflicts of Interest: The authors declare no conflict of interest.

References

- Zhang, G.; Yao, T.; Xie, H.; Zhang, K.; Zhu, F. Lakes' state and abundance across the Tibetan Plateau. *Chin. Sci. Bull.* **2014**, *59*, 3010–3021. [[CrossRef](#)]
- Wang, Z.; Schaaf, C.B.; Strahler, A.H.; Chopping, M.J.; Román, M.O.; Shuai, Y.; Woodcock, C.E.; Hollinger, D.Y.; Fitzjarrald, D.R. Evaluation of MODIS albedo product (MCD43A) over grassland, agriculture and forest surface types during dormant and snow-covered periods. *Remote Sens. Environ.* **2014**, *140*, 60–77. [[CrossRef](#)]
- Chen, Y.; Zong, Y.; Li, B.; Li, S.; Aitchison, J.C. Shrinking lakes in Tibet linked to the weakening Asian monsoon in the past 8.2 Ka. *Quat. Res.* **2013**, *80*, 189–198. [[CrossRef](#)]
- Zhang, G.; Xie, H.; Kang, S.; Yi, D.; Ackley, S.F. Monitoring lake level changes on the Tibetan Plateau using ICESat altimetry data (2003–2009). *Remote Sens. Environ.* **2011**, *115*, 1733–1742. [[CrossRef](#)]
- Wang, X.; Gong, P.; Zhao, Y.; Xu, Y.; Cheng, X.; Niu, Z.; Luo, Z.; Huang, H.; Sun, F.; Li, X. Water-level changes in China's large lakes determined from ICESat/GLAS data. *Remote Sens. Environ.* **2013**, *132*, 131–144. [[CrossRef](#)]
- Wan, W.; Long, D.; Hong, Y.; Ma, Y.; Yuan, Y.; Xiao, P.; Duan, H.; Han, Z.; Gu, X. A lake data set for the Tibetan Plateau from the 1960s, 2005, and 2014. *Sci. Data* **2016**, *3*. [[CrossRef](#)] [[PubMed](#)]
- Du, J.; Kimball, J.S.; Duguay, C.; Kim, Y.; Watts, J.D. Satellite microwave assessment of Northern Hemisphere lake ice phenology from 2002 to 2015. *Cryosphere* **2017**, *11*, 47–63. [[CrossRef](#)]
- Adrian, R.; O'Reilly, C.M.; Zagarese, H.; Baines, S.B.; Hessen, D.O.; Keller, W.; Livingstone, D.M.; Sommaruga, R.; Straile, D.; Van Donk, E. Lakes as sentinels of climate change. *Limnol. Oceanogr.* **2009**, *54*, 2283–2297. [[CrossRef](#)] [[PubMed](#)]
- Zhang, G.; Yao, T.; Xie, H.; Qin, J.; Ye, Q.; Dai, Y.; Guo, R. Estimating surface temperature changes of lakes in the Tibetan Plateau using MODIS LST data. *J. Geophys. Res. Atmos.* **2014**, *119*, 8552–8567. [[CrossRef](#)]
- Wang, S.-M.; Dou, H.S. *Lakes in China*; Science Press: Beijing, China, 1998.

11. Austin, J.A.; Colman, S.M. Lake Superior summer water temperatures are increasing more rapidly than regional air temperatures: A positive ice-albedo feedback. *Geophys. Res. Lett.* **2007**, *34*, 47–63. [[CrossRef](#)]
12. Hampton, S.E.; Izmest, E.; Lyubov, R.; Moore, M.V.; Katz, S.L.; Dennis, B.; Silow, E.A. Sixty years of environmental change in the world's largest freshwater lake—lake Baikal, Siberia. *Glob. Chang. Biol.* **2008**, *14*, 1947–1958. [[CrossRef](#)]
13. O'Reilly, C.M.; Sharma, S.; Gray, D.K.; Hampton, S.E.; Read, J.S.; Rowley, R.J.; Schneider, P.; Lenters, J.D.; McIntyre, P.B.; Kraemer, B.M. Rapid and highly variable warming of lake surface waters around the globe. *Geophys. Res. Lett.* **2015**, *42*. [[CrossRef](#)]
14. Ingram, W.; Wilson, C.; Mitchell, J. Modelling climate change: An assessment of sea ice and surface albedo feedbacks. *J. Geophys. Res. Atmos.* **1989**, *94*, 8609–8622. [[CrossRef](#)]
15. Efremova, T.; Pal'shin, N. Ice phenomena terms on the water bodies of Northwestern Russia. *Russ. Meteorol. Hydrol.* **2011**, *36*, 559–565. [[CrossRef](#)]
16. Guo, Z.; Wang, N.; Jiang, X.; Mao, R.; Wu, H. Research progress on snow and ice albedo measurement, retrieval and application. *Remote Sens. Technol. Appl.* **2013**, *28*, 739–746.
17. Bolsenga, S. Total albedo of great lakes ice. *Water Resour. Res.* **1969**, *5*, 1132–1133. [[CrossRef](#)]
18. Wiscombe, W.J.; Warren, S.G. A model for the spectral albedo of snow. I: Pure snow. *J. Atmos. Sci.* **1980**, *37*, 2712–2733. [[CrossRef](#)]
19. Heron, R.; Woo, M.-K. Decay of a high arctic lake-ice cover: Observations and modelling. *J. Glaciol.* **1994**, *40*, 283–292. [[CrossRef](#)]
20. Gardner, A.S.; Sharp, M.J. A review of snow and ice albedo and the development of a new physically based broadband albedo parameterization. *J. Geophys. Res. Earth Surf.* **2010**, *115*. [[CrossRef](#)]
21. Semmler, T.; Cheng, B.; Yang, Y.; Rontu, L. Snow and ice on Bear Lake (Alaska)—Sensitivity experiments with two lake ice models. *Tellus A Dyn. Meteorol. Oceanogr.* **2012**, *64*. [[CrossRef](#)]
22. Svacina, N.; Duguay, C.; Brown, L. Modelled and satellite-derived surface albedo of lake ice—Part I: Evaluation of the albedo parameterization scheme of the Canadian Lake Ice Model. *Hydrol. Process.* **2014**, *28*, 4550–4561. [[CrossRef](#)]
23. Shao, Z.-D.; Ke, C.-Q. Spring–summer albedo variations of Antarctic sea ice from 1982 to 2009. *Environ. Res. Lett.* **2015**, *10*. [[CrossRef](#)]
24. Svacina, N.; Duguay, C.; King, J. Modelled and satellite-derived surface albedo of lake ice—Part II: Evaluation of MODIS albedo products. *Hydrol. Process.* **2014**, *28*, 4562–4572. [[CrossRef](#)]
25. PÄRN, O.; Haapala, J. Occurrence of synoptic flaw leads of sea ice in the Gulf of Finland. *Boreal Environ. Res.* **2011**, *16*, 71–78.
26. Dirmhirn, I.; Eaton, F.D. Some characteristics of the albedo of snow. *J. Appl. Meteorol.* **1975**, *14*, 375–379. [[CrossRef](#)]
27. Warren, S.G. Optical properties of snow. *Rev. Geophys.* **1982**, *20*, 67–89. [[CrossRef](#)]
28. Bolsenga, S. Short note: Preliminary observations on the daily variation of ice albedo. *J. Glaciol.* **1977**, *18*, 517–521. [[CrossRef](#)]
29. Bolsenga, S. Spectral reflectances of snow and fresh-water ice from 340 through 1100 nm. *J. Glaciol.* **1983**, *29*, 296–305. [[CrossRef](#)]
30. Mullen, P.C.; Warren, S.G. Theory of the optical properties of lake ice. *J. Geophys. Res. Atmos.* **1988**, *93*, 8403–8414. [[CrossRef](#)]
31. Roesch, S.C. Modelling stress: A methodological review. *J. Behav. Med.* **1999**, *22*, 249–269. [[CrossRef](#)] [[PubMed](#)]
32. Hall, A.; Qu, X. Using the current seasonal cycle to constrain snow albedo feedback in future climate change. *Geophys. Res. Lett.* **2006**, *33*. [[CrossRef](#)]
33. Pirazzini, R. Challenges in snow and ice albedo parameterizations. *Geophysica* **2009**, *45*, 41–62.
34. Mallard, M.S.; Nolte, C.G.; Bullock, O.R.; Spero, T.L.; Gula, J. Using a coupled lake model with WRF for dynamical downscaling. *J. Geophys. Res. Atmos.* **2014**, *119*, 7193–7208. [[CrossRef](#)]
35. Ye, Q.; Wei, Q.; Hochschild, V.; Duguay, C.R. Integrated observations of lake ice at Nam Co. on the Tibetan Plateau from 2001 to 2009. In Proceedings of the 2011 IEEE International Geoscience and Remote Sensing Symposium (IGARSS), Vancouver, BC, Canada, 24–29 July 2011; pp. 3217–3220.
36. Huang, W.; Li, Z.; Han, H.; Niu, F.; Lin, Z.; Leppäranta, M. Structural analysis of thermokarst lake ice in Beiluhe Basin, Qinghai–Tibet Plateau. *Cold Reg. Sci. Technol.* **2012**, *72*, 33–42. [[CrossRef](#)]

37. Huang, W.; Han, H.; Shi, L.; Niu, F.; Deng, Y.; Li, Z. Effective thermal conductivity of thermokarst lake ice in Beiluhe Basin, Qinghai–Tibet Plateau. *Cold Reg. Sci. Technol.* **2013**, *85*, 34–41. [[CrossRef](#)]
38. Huang, W.; Li, R.; Han, H.; Niu, F.; Wu, Q.; Wang, W. Ice processes and surface ablation in a shallow thermokarst lake in the central Qinghai–Tibetan Plateau. *Ann. Glaciol.* **2016**, *57*, 20–28. [[CrossRef](#)]
39. Schaaf, C.B.; Gao, F.; Strahler, A.H.; Lucht, W.; Li, X.; Tsang, T.; Strugnell, N.C.; Zhang, X.; Jin, Y.; Muller, J.-P. First operational BRDF, albedo nadir reflectance products from MODIS. *Remote Sens. Environ.* **2002**, *83*, 135–148. [[CrossRef](#)]
40. Liu, Y.; Sun, Q.; Wang, Z.; Schaaf, C.; Erb, A. Evaluation of VIIRS daily BRDF, albedo, and NBAR product using the MODIS collection V006 product and in situ measurements. In Proceedings of the 2016 IEEE International Geoscience and Remote Sensing Symposium (IGARSS), Beijing, China, 10–15 July 2016; pp. 1962–1965.
41. Hall, D.K.; Riggs, G.A. Accuracy assessment of the MODIS snow products. *Hydrol. Process.* **2007**, *21*, 1534–1547. [[CrossRef](#)]
42. Crosman, E.T.; Horel, J.D. MODIS-derived surface temperature of the Great Salt Lake. *Remote Sens. Environ.* **2009**, *113*, 73–81. [[CrossRef](#)]
43. Song, X.; Wang, Y.; Tang, B.; Leng, P.; Sun, C.; Peng, J.; Loew, A. Estimation of land surface temperature using FengYun-2E (FY-2E) data: A case study of the source area of the yellow river. *IEEE J. Sel. Top. Appl. Earth Obs. Remote Sens.* **2017**, *10*, 1–8. [[CrossRef](#)]
44. Mironov, D.; Ritter, B. *A New Sea Ice Model for GME*; Technical Note; Deutscher Wetterdienst: Offenbach am Main, Germany, 2004.
45. Subin, Z.M.; Riley, W.J.; Mironov, D. An improved lake model for climate simulations: Model structure, evaluation, and sensitivity analyses in CESM1. *J. Adv. Model. Earth Syst.* **2012**, *4*. [[CrossRef](#)]
46. Mironov, D. *Parameterization of Lakes in Numerical Weather Prediction. Part 1: Description of a Lake Model*. Offenbach: Consortium for Small-Scale Modelling; Technical Report 11; Deutscher Wetterdienst: Offenbach am Main, Germany, 2003.
47. Mironov, D.; Heise, E.; Kourzeneva, E.; Ritter, B.; Schneider, N.; Terzhevik, A. Implementation of the lake parameterisation scheme FLake into the numerical weather prediction model COSMO. *Boreal Environ. Res.* **2010**, *15*, 218–230.
48. Perroud, M.; Goyette, S.; Martynov, A.; Beniston, M.; Annevillec, O. Simulation of multiannual thermal profiles in deep Lake Geneva: A comparison of one-dimensional lake models. *Limnol. Oceanogr.* **2009**, *54*, 1574–1594. [[CrossRef](#)]
49. Kheyrollah Pour, H.; Duguay, C.; Martynov, A.; Brown, L. Simulation of surface temperature and ice cover of large northern lakes with 1-D models: A comparison with MODIS satellite data and in situ measurements. *Tellus A Dyn. Meteorol. Oceanogr.* **2012**, *64*. [[CrossRef](#)]
50. Stepanenko, V.; Jöhnk, K.D.; Machulskaya, E.; Perroud, M.; Subin, Z.; Nordbo, A.; Mammarella, I.; Mironov, D. Simulation of surface energy fluxes and stratification of a small boreal lake by a set of one-dimensional models. *Tellus A Dyn. Meteorol. Oceanogr.* **2014**, *66*. [[CrossRef](#)]
51. Gou, P.; Ye, Q.; Wei, Q. Lake ice change at the Nam Co. Lake on the Tibetan Plateau during 2000–2013 and influencing factors. *Prog. Geogr.* **2015**, *34*, 1241–1249.
52. Bengtsson, L. Spatial variability of lake ice covers. *Geogr. Ann. Ser. A Phys. Geogr.* **1986**, *68*, 113–121. [[CrossRef](#)]
53. Petrov, M.; Terzhevik, A.Y.; Palshin, N.; Zdorovenov, R.; Zdorovenova, G. Absorption of solar radiation by snow-and-ice cover of lakes. *Water Resour.* **2005**, *32*, 496–504. [[CrossRef](#)]
54. Jakkila, J.; Leppäranta, M.; Kawamura, T.; Shirasawa, K.; Salonen, K. Radiation transfer and heat budget during the ice season in Lake Pääjärvi, Finland. *Aquat. Ecol.* **2009**, *43*, 681–692. [[CrossRef](#)]
55. Bernhardt, J.; Engelhardt, C.; Kirillin, G.; Matschullat, J. Lake ice phenology in Berlin-Brandenburg from 1947–2007: Observations and model hindcasts. *Clim. Chang.* **2012**, *112*, 791–817. [[CrossRef](#)]
56. Salonen, K.; Pulkkanen, M.; Salmi, P.; Griffiths, R.W. Interannual variability of circulation under spring ice in a boreal lake. *Limnol. Oceanogr.* **2014**, *59*, 2121–2132. [[CrossRef](#)]
57. Van Cleave, K.; Lenters, J.D.; Wang, J.; Verhamme, E.M. A regime shift in Lake Superior ice cover, evaporation, and water temperature following the warm El Niño winter of 1997–1998. *Limnol. Oceanogr.* **2014**, *59*, 1889–1898. [[CrossRef](#)]

58. Donlon, C.J.; Minnett, P.J.; Gentemann, C.; Nightingale, T.J.; Barton, I.J.; Ward, B.; Murray, M.J. Toward improved validation of satellite sea surface skin temperature measurements for climate research. *J. Clim.* **2001**, *15*, 353–369. [[CrossRef](#)]
59. Schaaf, C.; Wang, Z.; Shuai, Y.; Strahler, A. Daily operational MODIS BRDF, albedo and nadir reflectance products (V006). In Proceedings of the AGU Fall Meeting Abstracts, San Francisco, CA, USA, 3–7 December 2012.
60. Chen, A.; Liang, X.; Bian, L.; Liu, Y. Analysis on MODIS albedo retrieval quality over the Qinghai-Tibet Plateau. *Plateau Meteorol.* **2016**, *35*, 277–284.



© 2018 by the authors. Licensee MDPI, Basel, Switzerland. This article is an open access article distributed under the terms and conditions of the Creative Commons Attribution (CC BY) license (<http://creativecommons.org/licenses/by/4.0/>).